Geophys. J. Int. (2009) doi: 10.1111/j.1365-246X.2009.04092.x

Mantle transition zone structure beneath Kenya and Tanzania: more evidence for a deep-seated thermal upwelling in the mantle

Audrey D. Huerta,[1] Andrew A. Nyblade[2] and Angela M. Reusch[2]

[1]*Department of Geological Sciences, Central Washington University, Ellensburg,* WA 98926, *USA. E-mail: huerta@geology.cwu.edu*
[2]*Department of Geosciences, Pennsylvania State University, University Park,* PA 16802, *USA*

Accepted 2009 January 7. Received 2008 October 17; in original form 2008 March 31

SUMMARY

Here we investigate the thermal structure of the mantle beneath the eastern Branch of the East African Rift system in Kenya and Tanzania. We focus on the structure of the mantle transition zone, as delineated by stacking of receiver functions. The top of the transition zone (the 410 km discontinuity) displays distinctive topography, and is systematically depressed beneath the rift in Kenya and northern Tanzania and adjacent volcanic fields. This depression is indicative of a localized ~350 °C thermal anomaly. In contrast, the bottom of the transition zone (the 660 km discontinuity) is everywhere depressed. This region-wide depression is best explained as a *Ps* conversion from the majorite–perovskite transition of anomalously warm mantle. We interpret this structure of the transition zone as resulting from the ponding of a mantle plume (possibly the deep-mantle African Superplume) at the base of the transition zone, which then drives localized thermal upwellings that disrupt the top of the transition zone and extend to shallow mantle depths beneath the rift in Kenya and northern Tanzania.

Key words: Mantle processes; Hotspot; Africa.

1 INTRODUCTION

The Cenozoic East African rift system is a classic example of a continental rift; exhibiting characteristic patterns of rifting, volcanism and plateau uplift. The location of the rift is strongly controlled by Precambrian tectonics, with both the eastern and western branches following Proterozoic mobile belts that wrap around the Archean Tanzania Craton (Fig. 1; e.g. Ebinger 1989; Hetzel & Strecker 1994; Tesha *et al.* 1997; Nyblade & Brazier 2002). The eastern branch of the rift has been studied more extensively than the western branch, and a general progression of volcanic activity related to the rifting is thought to have migrated from north to south with volcanism starting at *ca.* 30 Ma in northern Kenya, at *ca*. 20 Ma in central Kenya, at *ca*. 12 Ma in southern Kenya and at *ca*. 8 Ma in northern Tanzania (George *et al.* 1998).

Many seismic studies of mantle structure beneath eastern Africa have delineated velocity anomalies spatially coincident with the surface expression of the volcanism, plateau uplift, and rift faulting (e.g. Prodehl *et al.* 1994; Fuchs *et al.* 1997; Nyblade & Brazier 2002, and references therein). Beneath the eastern branch in Tanzania, tomographic models show a low velocity zone (LVZ) extending at least to depths of ~400 km (Ritsema *et al.* 1998; Weeraratne *et al.* 2003), and in Kenya the work of Park & Nyblade (2006) reveals a LVZ extending to at least 300 km depth. In both Tanzania and Kenya, the LVZ dips westward beneath the Tanzania Craton at depths >200 km, while above ~200 km depth the LVZ is centred beneath the rift structures. Receiver function stacks of the mantle beneath the eastern branch in Tanzania reveal a 20–30 km deep depression of the 410 km discontinuity coincident with the location of the LVZ, confirming that at least part of the LVZ is caused by elevated rock temperatures (Nyblade *et al.* 2000; Owens *et al.* 2000).

The origin of the anomalous upper-mantle structure under east Africa remains uncertain, largely because in many areas its lateral and depth extent are unknown. Plume models have been invoked as an explanation (e.g. Burke 1996; Ebinger & Sleep 1998; George *et al.* 1998; Nyblade *et al.* 2000), including the possibility that the anomalous upper-mantle structure is linked geodynamically to the African Superplume, a large thermal and chemical anomaly in the lower mantle centred beneath southern Africa (e.g. Ritsema *et al.* 1999; Simmons *et al.* 2007). However, non-plume models have also been suggested (e.g. King & Ritsema 2000). Critical to discerning the origin of the upper-mantle anomaly is a clearer picture of its shape, both laterally and vertically.

In response to this need, here we image the structure of the mantle transition zone beneath Kenya, and combine our images with previously mapped mantle transition zone structure in Tanzania (Fig 1). To do this, we stack *P*-to-*S* converted phases seen in receiver functions to map topography of the phase transitions that nominally occur at depths of 410 and 660 km. The 410 and 660 km discontinuities, which bound the transition zone, are generally interpreted as the α-olivine->β-spinel transition and the γ-spinel->perovskite+magnesiouwustite transition, respectively (Bina & Helffrich 1994). The Clapeyron slope of these transitions is such that under warm conditions the 410 transition is depressed and the 660 transition is elevated, and the thickness of the transition

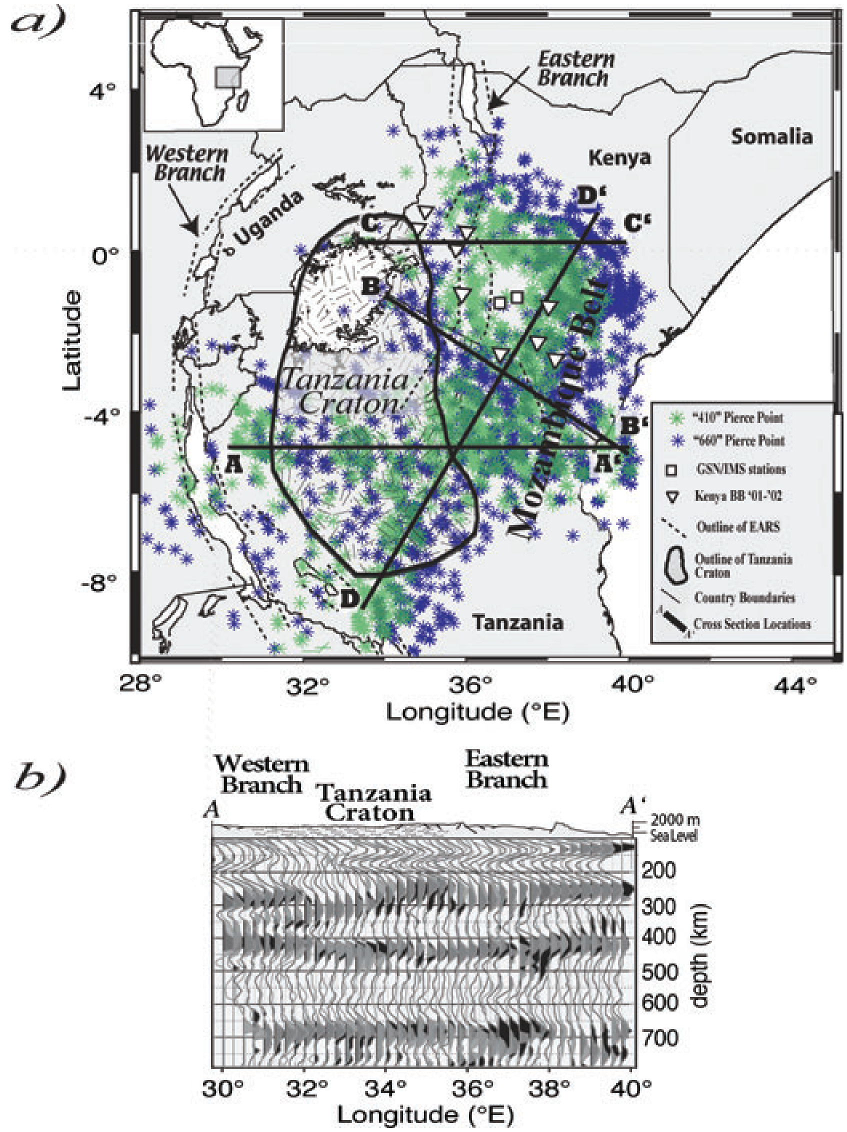

Figure 1. (a) Map of study area showing major geologic features of the East African Rift System and Tanzania Craton, distribution of piercing points, and locations of cross-sections A–A′ (above), B–B′, C–C′ and D–D′ (Fig. 2) (b) Cross-section A–A′ at ∼4.5°S comparing receiver functions based on IASP91 2-D earth model (grey, this work) and receiver functions based on 3-D earth model (black, Owens *et al.* 2000). In this figure all stacks are based on the same criteria as those of Owens *et al.* (2000), i.e. 1-deg. bin radius, and minimum of four stations and 30 events.

zone decreases. Our results yield new constraints on the extent of the thermal anomaly under the eastern branch, providing observations valuable to understanding the thermal and dynamic nature of the mantle beneath the rift.

2 METHODOLOGY

For this study, we analyse teleseismic receiver functions obtained from seismograms recorded by the 2000–2002 Kenya Broadband Seismic Experiment (Nyblade & Langston 2002), permanent IRIS/GSN stations in Kenya (KMBO, 1995–2006; NAI, 1995) and the 1994–1995 Tanzania Broadband Seismic Experiment (Nyblade *et al.* 1996). Data used for this study came from earthquakes with $M_b > 5.5$ and located at a distance from the stations between 30° and 90° for the *Ps* phase and a distance between 90° and 120° for the *PPs* phase. The data coverage is illustrated in Fig. 1.

For processing the data, we used the same methods and parameters as (Owens *et al.* 2000) so that we could compare directly our results with their results from Tanzania. We calculated receiver functions using frequency domain deconvolution with water stabilization and a Gaussian filter of 0.4 (Langston 1979; Ammon 1991). We then determined theoretical *Ps–P* arrival times using the 1-D IASP91 velocity model (Kennett & Engdahl 1991) for each event-station pair. This theoretical arrival time was used to assign a specific traveltime and associated amplitude in 10 km vertical increments. The amplitudes from the appropriate *Ps–P* time for each receiver function between 40 and 800 km depth were then binned and summed to create receiver function stacks.

We had to resort to using a 1-D velocity model for this study (IASP91; Kennett & Engdahl 1991) since there is only a *P*-wave model available for Kenya (Park & Nyblade 2006). To examine the influence of using the 1-D velocity model versus a 3-D model on the receiver function stacks, we compared our stacked receiver functions using a 1-D model with receiver function stacks previously generated by Owens *et al.* (2000) using a 3-D *P*- and *S*-wave velocity model for Tanzania (Ritsema *et al.* 1998) (Fig. 1b). Results of this comparison show minimal differences: the receiver function stacks generated with the 1-D model match the stacks from the 3-D model quite well (Fig. 1b). Both methods yield similar *Ps* conversions from depths of ∼250, ∼410 and ∼660 km, and in particular, results from both methods show a similar 20–30 km deep depression of the 410 discontinuity between ∼32° and 37°E. Thus, we conclude that receiver functions based on the 1-D velocity model adequately capture the salient geometry of the mantle beneath in this region.

To obtain receiver function stacks with the best possible signal-to-noise ratios but still maintain the ability to resolve variations in discontinuity topography over horizontal distances of about 100 km, we found that the optimal stacking parameters included a minimum of seven receiver functions per bin from at least three stations, a bin radius of 1.25°, and a bin increment of 0.25°.

Owens *et al.* (2000) found that, for their method of stacking receiver functions with a fixed velocity model, the precision of the depth estimate of the discontinuities was on the order of ±3 km. However, because of our 10 km vertical binning, uncertainties in crustal thickness (e.g. Prodehl *et al.* 1994; Fuchs *et al.* 1997, and references therein) and upper-mantle velocities (Slack *et al.* 1994; Achauer & Masson 2002; Park & Nyblade 2006) for our study area, we estimate the uncertainties in our discontinuity depths to be ±10 km. In addition, the combination of parameters used results in variable vertical smoothing of the signal over >10 km, and thus we focus on the maxima of the arrival peaks rather than the upper limits.

3 RESULTS

Shown in Fig. 2 are three profiles that illustrate our major findings. In general, we see significant variations in the depth and characteristics of the 410 km discontinuity, while there is less variability in the depth of the 660 km discontinuity throughout the region. Profile B–B′, which runs almost parallel to the Kenya–Tanzania border, shows strong and coherent *Ps* conversions from the 410 and 660 km discontinuities (Fig. 2). In the west-most region, beneath the Tanzania Craton, a clear *Ps* arrival can be seen at a depth of ∼410–420 km. Across the central portion of profile B–B′ (beneath the rift and the volcanic fields east of the rift) this *Ps* arrival shifts deeper to ∼430–450 km depth. And, in the southeast portion of profile B–B′ (beneath the coastal plains) the P410s shallows again to ∼410–420 km depth. This 30–40 km depression of the 410 km discontinuity is similar in character (depth and breadth) to the depression of the 410 km discontinuity seen in Tanzania to the south (Fig. 1b).

Profile C–C′, which crosses Kenya west to east at the equator, also shows a clear P410s arrival at a depth of 410–420 km beneath the Tanzania Craton (Fig. 2). And, similar to profile B–B′, the P410s arrival is depressed by 30–40 km to the east of the Kenya rift beneath the area of off-axis volcanism (Mt Kenya). However, in this profile, the P410s arrival is not clearly seen beneath the rift. Profile D–D′ crosses east Africa from southwest to northeast, extending from the western branch in the south, across the Tanzania Craton, and into the eastern branch (Fig. 2). As in other profiles, a clear *Ps* arrival can be seen beneath the craton at a depth of ∼410 km. The P410s arrival is depressed by about ∼20 km beneath the western branch and by 30–40 km beneath the eastern branch, relative to the P410s arrival beneath the Tanzania Craton.

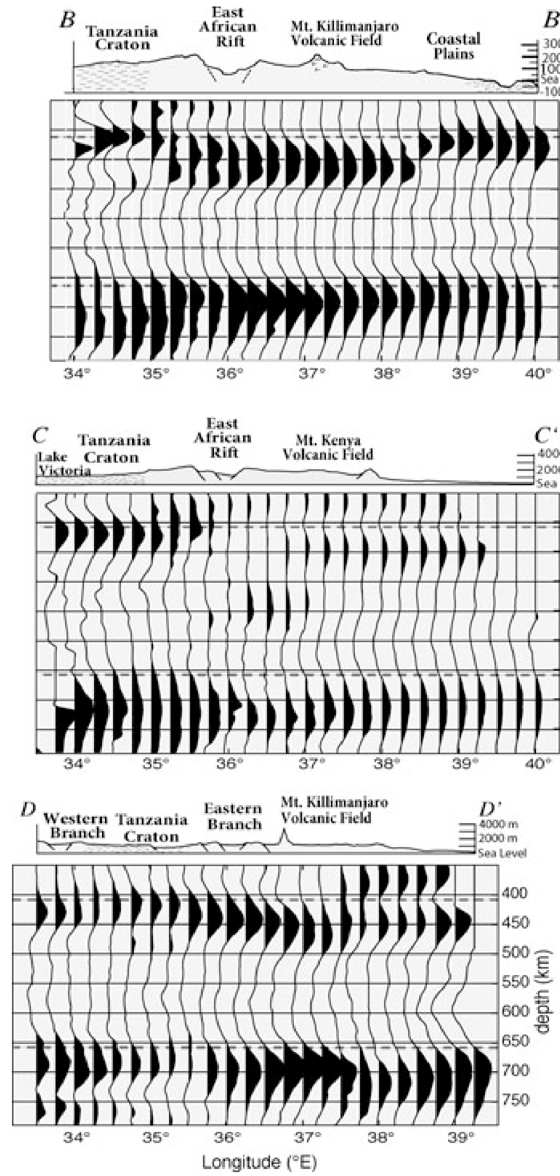

Figure 2. Receiver function cross-sections displaying structure of mantle transition zone and surface geology. Stacking parameters: a minimum of seven receiver functions per bin from at least three stations, a bin radius of 1.25°, and a bin increment of 0.25°.

In all cross-sections, the 660 km discontinuity displays minimal topography across the entire region (Fig. 2). This is in marked contrast to the 30–40 km of relief observed on the 410 km discontinuity. The P660s arrival is characterized by a broad arrival that is everywhere depressed, with a maximum amplitude at a depth between 680 and 700 km. What little topography that is seen falls within the ±10 km uncertainty of our results. A similar observation was made for the P660s arrival in Tanzania by Owens *et al.* (2000), but they did not provide an interpretation for why the 660 km discontinuity could be flat across the region and deeper than expected.

Fig. 3 displays the depth of the P410s and P660s discontinuities throughout the region. Consistent with the profiles in Fig. 2, there is a strong correlation between the depth to the P410s and surface geology. Beneath the Tanzania Craton, the P410s arrival is consistently seen at depths of 410–420 km. In contrast, the P410s arrival from beneath the rift and the off-axis volcanic fields to the

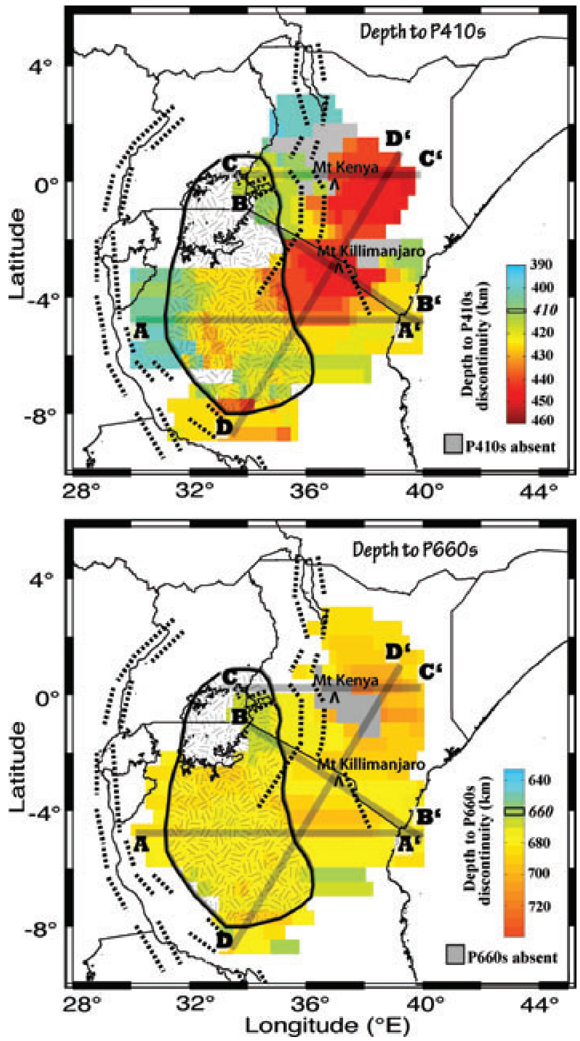

Figure 3. Lateral and vertical extent of anomalous mantle. Map views showing depth of the P410s and P660s arrivals in relation to geologic features in East Africa. Grey squares denote regions without resolvable P410s or P660s arrivals. Hatchered region denotes surficial extent of Tanzania Craton, dashed lines outline major Cenozoic rift faults, major volcanoes as indicated.

east is depressed, seen at depths of 430–450 km. Areas lacking clear P410s arrivals, for example under some parts of the Kenya rift, are found where the P410s abruptly transitions from shallower to deeper depths. This pattern is consistent with previous studies showing that topography on discontinuities can lead to scattering and interference patterns that can greatly modify the amplitude of the *Ps* conversion, and in fact, can result in receiver function stacks that show no clear *Ps* conversion (Vanderlee *et al.* 1994). Again, consistent with the profiles of Fig. 2, the P660s arrival is everywhere depressed, occurring at depths of ∼680 km beneath most of the region and occurring at even greater depths beneath the portions of the eastern branch and the adjacent volcanic fields.

4 DISCUSSION

In summary, we find that the depth of the 410 km discontinuity is systematically depressed by 30–40 km within the study region. It is at a depth of 410–420 km beneath the Tanzania Craton and at a depth of 430–450 km beneath the eastern branch of the rift system and the adjacent off-axis volcanism. By contrast, the depth of the 660 km discontinuity does not vary significantly, but it is everywhere deeper than normal. The amplitude of the P660s arrival commonly peaks at depths of ∼680 km, with infrequent peaks at greater depths. This documentation of a pervasive presence of a depressed 660 km discontinuity beneath a region with a locally depressed 410 km discontinuity that correlates with the rifting and volcanism in the eastern branch is a new observation, and one that potentially places important constraints on the nature of perturbed mantle structure beneath east Africa.

We attribute the locally depressed 410 km discontinuity to warmer-than-average temperatures at the top of the transition zone beneath the rift and the off-axis volcanism, consistent with the interpretation of Owens *et al.* (2000). Using a Clapeyron slope of 2.9 MPa K^{-1} (Bina & Helffrich 1994) for the α-olivine to β-spinel transition, the 30–40 km depression of the 410 km corresponds to a ∼350 °C increase in temperature. This increase in temperature is consistent with the velocity model of Ritsema *et al.* (1998), which shows a 2–3 per cent reduction in *S*-wave velocities beneath the eastern branch coincident with the location of the depressed 410 km discontinuity in Tanzania. This distinct 200–300 km wide thermal anomaly at the top of the transition zone must be accounted for by any plausible geodynamic explanations for the origin of Cenozoic extensional tectonism in East Africa.

The flat and pervasively depressed 660 km discontinuity is far broader than the Fresnel zone diameter of ∼200 km (Sheriff 1980), and is more difficult to explain. We offer three possible interpretations. First, there may be a systematic error in our stacking of the receiver functions that leads to a depressed P660s arrival everywhere. This could possibly be the result of lower-than-average wave speeds within or above the transition zone that are not properly accounted for in the stacking procedure. For example, a uniform >7 per cent reduction of the modelled velocity across the entire transition zone would depress the calculated depth of the P660s from 660 to 680 km. However, observed velocities variations in the region are not continuous, with maximum localized anomalies of ±3 per cent (Ritsema *et al.* 1998). Additionally, we note that our depressed P660s matches the location of the P660s calculated with the 3-D velocity model of Owens *et al.* (2000). We also note that there is no correlative systematic shift of the P410s arrivals, and that the 410 km discontinuity beneath the Tanzania Craton is at a normal depth. Thus, we do not think that there are significant errors in our traveltime to depth calculations, and that the flat and depressed 660 km discontinuity is not an artefact of the 1-D velocity models used in the stacking.

A second possibility is that there is colder-than-normal mantle at the base of the transition zone, with warmer-than-normal mantle at the top of the transition zone. This interpretation follows from the assumption that the observed P410s and the P660s arrivals are the result of olivine-spinel phase transformations as summarized in the introduction (Bina & Helffrich 1994). We do not favour this interpretation because no plausible mechanisms can explain an inverted thermal anomaly in the transition zone beneath eastern Africa. For example, a common way to create cool temperatures within the lower transition zone is through the emplacement of cold subducted lithosphere, but there has not been any subduction beneath east Africa for *ca*. 500 Ma. Likewise, we discount the foundering of a cold cratonic keel as a viable mechanism for cooling the lower transition zone since seismic images of the lithosphere under the Tanzania Craton indicate that the keel is more or less intact (Ritsema *et al.* 1999; Weeraratne *et al.* 2003). Thus, we argue that the cool lower-mantle scenario is highly implausible in light of

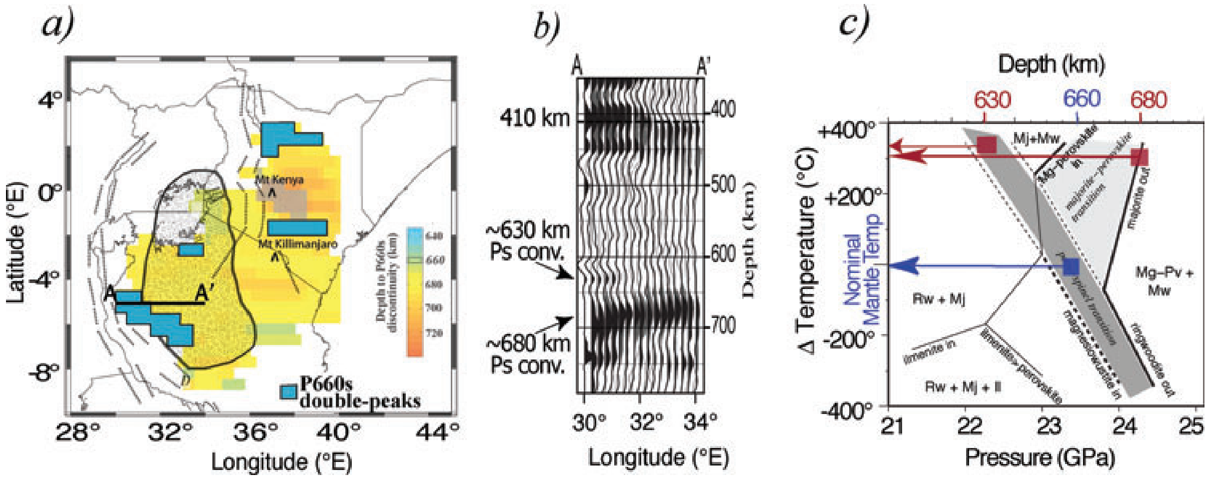

Figure 4. Observations and interpretations of double *Ps* arrivals near depths of 660 km. (a) Map view showing regions where double arrivals are observed in the high-frequency stacks (blue polygons) overlain on 660-depth map. (b) Cross-section A–A′ displaying the double *Ps* arrivals observed in the high frequency stacks (black; Gaussian = 1.5) overlain on the low-frequency stacks (grey; Gaussian = 0.4). Stacking parameters: a minimum of seven receiver functions per bin from at least three stations, a bin radius of 1.25°, and a bin increment of 0.25°. (c) Phase diagram showing P–T conditions for the majorite –> perovskite and post- spinel transitions. Red squares display estimated temperatures at the depths of the observed double arrivals in cross-section A–A′ (after Hirose 2002).

the known tectonic history of the region and the seismic structure of the upper mantle.

A third possible interpretation for the depressed 660 km discontinuity under east Africa is that the P660s arrival is a *Ps* conversion from the majorite (garnet)–> perovskite + magnesiouwustite transition and not the γ-spinel (olivine) –> perovskite + magnesiouwustite transition. Recent mineral physics studies indicate that there can be multiple phase transitions in a pyrolitic mantle at depths of ∼660 km, complicating the interpretation of seismic wave conversions from that depth (Vacher *et al.* 1998; Simmons & Gurrola 2000; Hirose 2002; Deuss *et al.* 2006; Deuss 2007). In particular, the depth of the majorite–perovskite transition can occur at depths of ∼660 km (Hirose 2002). The majorite–perovskite transition has a positive Clapeyron slope, and thus the transition deepens with increasing temperature. Indeed, recent investigations of 'hotspot' receiver functions indicate that in areas of elevated temperature the majorite–perovskite transition may be the dominant discontinuity, resulting in deeper than average P660s signals (Deuss 2007).

In some instances, both discontinuities have been imaged, resulting in double *Ps* arrivals at the base of the transition zone (Simmons & Gurrola 2000; Deuss *et al.* 2006; Deuss 2007). While low-frequency receiver functions (Gaussian filter of 0.4) presented here do not reveal double *Ps* arrivals, we inspected high-frequency receiver functions (Gaussian filter of 1.5) across the study area. Even at the higher frequency, most of the receiver functions throughout the region display only the single deep and broad *Ps* arrival. However, we observe the occasional occurrence of double arrivals. These double arrivals are clustered in distinct subregions beneath the Tanzania Craton and the off-axis volcanic fields (Fig. 4a). For example, Fig. 4(b) displays a typical occurrence of the double arrival (between latitudes of 30°E and 31.5°E) with a distinct upper arrival at depths of ∼630 km and a relatively broad lower arrival with maximum amplitude at a depth of ∼680 km. If, indeed, the upper arrival is a conversion off of the post-spinel transition, and the lower arrival is a conversion off of the majorite –> perovskite transition, then these depths could be used to estimate the thermal condition of the mantle in these regions. In the regions displaying the double arrivals with typical depths of ∼630 km and ∼680 km, both the post-spinel and the majorite-out transitions suggest thermal anomalies ∼300 °C (Hirose 2002). However, note that even though these two temperature estimates are self-consistent, estimates of temperature anomalies based on the majorite > perovskite transition depth are uncertain since this transition is highly sensitive to mantle chemistry (Hirose 2002).

While we acknowledge that there is still much uncertainty in how to interpret *Ps* arrivals from the base of the mantle transition zone, we argue that an interpretation attributing the depressed 660 km discontinuity observed throughout Kenya and Tanzania to *Ps* conversions from the majorite-out transition at elevated temperatures is a reasonable interpretation. This interpretation invokes the presence of a thermal anomaly at the base of the transition zone that is much broader than the thermal anomaly at the top of the transition zone, extending across all of east Africa (∼1000 to 1500 km wide).

How might such a broad thermal anomaly form within the base of the mantle transition zone? A broad thermal anomaly could not be generated by the commonly invoked plume structure of a bulbous head fed by a narrow tail (100–200 km wide) (Griffiths & Campbell 1990), which many authors call upon to explain the Cenozoic tectonism in east Africa (e.g. Burke 1996; Ebinger & Sleep 1998; George *et al.* 1998; Nyblade *et al.* 2000). However, recent geodynamic studies of mantle processes that incorporate more detailed physics, chemistry and boundary conditions into their models are producing plumes that do not develop the classic head and tail structures (e.g. Lin & van Keken 2006; Campbell 2007; Farnetani & Hofmann 2007). Rather, these models predict a variety of plume shapes and sizes with complex dynamics that often pond at the base of the mantle transition zone (Farnetani & Hofmann 2007). The modelled plumes arise from anomalies at the core–mantle boundary and can develop irregular shapes extending high into the mantle, creating broad thermal anomalies leading to smaller convective instabilities within the lower part of the transition zone that upwell towards the surface.

The ponding of such plume material at the base of the mantle transition zone may explain the regionally depressed 660 km discontinuity observed beneath east Africa, provided that the depressed 660 km discontinuity results from the majorite to perovskite transition. And a smaller, secondary thermal upwelling originating

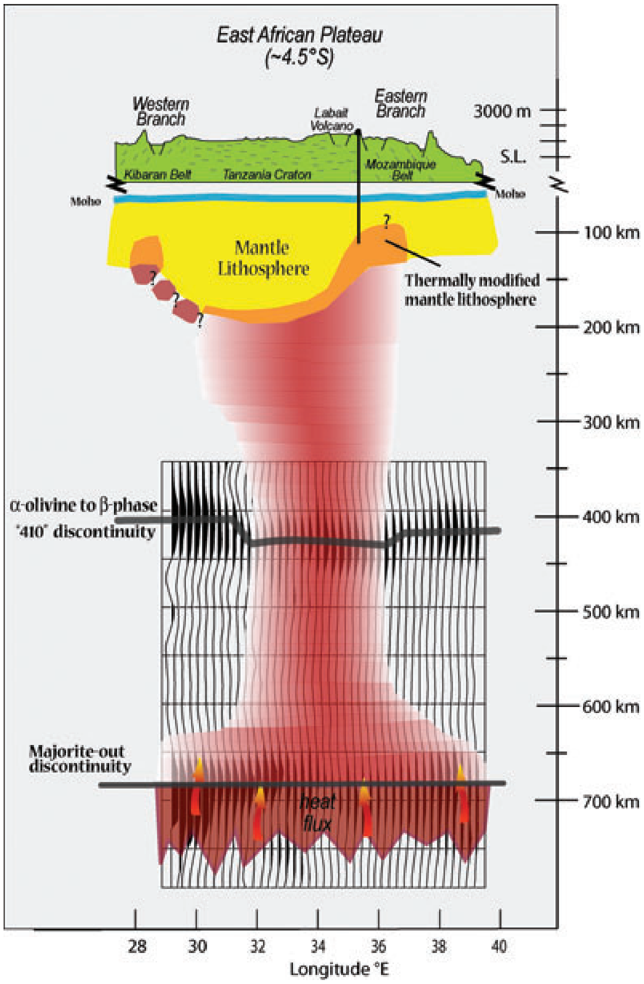

Figure 5. Schematic cross-section at ∼4.5°S showing receiver function stacks of mantle transition zone and cartoon of the associated thermal upwelling. The region-wide *Ps* conversion at ∼680 km arises from the majorite-out discontinuity of mantle heated by ponding of the plume at the base of the transition zone. The localized *Ps* conversion at ∼430 km results from the α-olivine to β-spinel discontinuity of thermally upwelling mantle. Question marks beneath eastern and western rifts indicate that structures illustrated are poorly determined. Updated from Nyblade *et al.* (2000).

from the base of the transition zone could account for the narrower thermal anomaly at the top of the transition zone creating the 30–40 km deep depression of the 410 km discontinuity.

We have illustrated this interpretation schematically in Fig. 5 by altering the mantle plume model from Nyblade *et al.* (2000), which showed a plume head rising beneath the eastern side of the Tanzania Craton, and warm plume head material flowing up the sides of the thick cratonic lithosphere perturbing lithospheric structure under the eastern and western branches of the rift system. In Fig. 5, we essentially keep the structure above 250 km depth the same as in the Nyblade *et al*. cartoon, but at deeper depths we show (1) a broad thermal anomaly at the base of the transition zone and (2) a narrower thermal upwelling rising through the transition zone and impinging on the base of the cratonic lithosphere. The thermal upwelling crosses the 410 km discontinuity in the region where this discontinuity is depressed.

There has been considerable discussion recently about the possible connectivity between the lower-mantle African Superplume and the anomalous upper-mantle structure under east Africa (Ritsema *et al.* 1999; Benoit *et al.* 2006; Montelli *et al.* 2006; Park & Nyblade 2006; Pik *et al.* 2006; Simmons *et al.* 2007). Our favoured interpretation (Fig. 5) is consistent with a through-going mantle anomaly, but one that does not require a flux of mantle rock across the 660 km discontinuity. The depressed 660 km discontinuity that we image could simply result from the diffusion of heat from the lower to the upper mantle within the African Superplume. Additionally, there has also been considerable discussion about multiple plumes in the upper mantle beneath east Africa(e.g. George *et al.* 1998; Furman *et al.* 2006; Pik *et al.* 2006). Our interpretation of a broad thermal anomaly at the base of the mantle transition zone could be fertile grounds for spawning more than one thermal upwelling, and could explain various geochemical and/or geophysical anomalies indicating multiple plumes.

5 SUMMARY

Stacks of receiver functions throughout Kenya and Tanzania reveal that the top of the transition zone (the 410 km discontinuity) is locally depressed beneath the Eastern Branch of the East African Rift system and off-axis volcanism, indicating a mantle thermally perturbed by ∼350 °C. The bottom of the transition zone (the 660 km discontinuity) is uniformly depressed throughout the ∼600 000 km^2 area. This region-wide depression can be interpreted as a *Ps* conversion from majorite-to-perovskite transition, indicating pervasively warm mantle. We interpret the structure of the transition zone as the result of ponding of a thermal-chemical plume at the base of the transition zone driving a localized thermal upwelling that rises around the margins of the Tanzania Craton.

ACKNOWLEDGMENTS

We are grateful for software made available by Chuck Ammon and Tom Owens, and helpful discussions with Jordi Julia and Garrett Ito. We would also like to thank two anonymous reviewers for their helpful comments. This research was funded by National Science Foundation grants #0003424 and #0530062.

REFERENCES

Achauer, U. & Masson, F., 2002. Seismic tomography of continental rifts revisited: from relative to absolute heterogeneities, *Tectonophysics,* **358**(1–4), 17–37.

Ammon, C.J., 1991. The isolation of receiver effects from teleseismic P-wave-forms, *Bull. seism. Soc. Am.,* **81**(6), 2504–2510.

Benoit, M.H., Nyblade, A.A. & VanDecar, J.C., 2006. Upper mantle P-wave speed variations beneath Ethiopia and the origin of the Afar hotspot, *Geology,* **34**(5), 329–332.

Bina, C.R. & Helffrich, G., 1994. Phase-transition Clapeyron slopes and transition zone seismic discontinuity topography, *J. Geophys. Res.-Solid Earth,* **99**(B8), 15 853–15 860.

Burke, K., 1996. The African Plate, *S. Afric. J. Geol.,* **99**(4), 341–409.

Campbell, I.H., 2007. Testing the plume theory, *Chem. Geol.,* **241**(3-4), 153–176, Sp. Iss. SI.

Deuss, A., 2007. Seismic observations of transition zone discontinuities beneath hotspot locations, in *Plates, Plumes, and Planetary Processes,* Vol. Special Paper 430, pp. 121–136, eds Foulger, G. & Jurdy, D., Geological Society of America.

Deuss, A., Redfern, S.A.T., Chambers, K. & Woodhouse, J.H., 2006. The nature of the 660-kilometer discontinuity in Earth's mantle from global seismic observations of PP precursors, *Science,* **311**(5758), 198–201.

Ebinger, C.J., 1989. Geometric and kinematic development of border faults and accommodation zones, Kivu-Rusizi Rift, Africa, *Tectonics,* **8**(1), 117–133.

Ebinger, C.J. & Sleep, N.H., 1998. Cenozoic magmatism throughout east Africa resulting from impact of a single plume, *Nature,* **395**(6704), 788–791.

Farnetani, C.G. & Hofmann, A.W., 2007. Dynamics and internal structure of mantle plume conduit, *Geochim. Cosmochim. Acta,* **71**(15), A268–A268, Suppl. S.

Fuchs, K., Altherr, R., Muller, B. & Prodehl, C., 1997. *Structure and Dynamic Processes in the Lithosphere of the Afro-Arabian Rift System,* Vol. 278, Tectonophysics, Elsevier, Amsterdam.

Furman, T., Kaleta, K.M., Bryce, J.G. & Hanan, B.B., 2006. Tertiary mafic lavas of Turkana, Kenya: constraints on East African plume structure and the occurrence of high-mu volcanism in Africa, *J. Petrol.,* **47**(6), 1221–1244.

George, R., Rogers, N. & Kelley, S., 1998. Earliest magmatism in Ethiopia: evidence for two mantle plumes in one flood basalt province, *Geology,* **26**(10), 923–926.

Griffiths, R.W. & Campbell, I.H., 1990. Stirring and structure in mantle starting plumes, *Earth planet. Sci. Lett.,* **99**(1–2), 66–78.

Hetzel, R. & Strecker, M.R., 1994. Late Mozambique Belt structures in western Kenya and their influence on the evolution of the Cenozoic Kenya Rift, *J. Struct. Geol.,* **16**(2), 189–201.

Hirose, K., 2002. Phase transitions in pyrolitic mantle around 670-km depth: Implications for upwelling of plumes from the lower mantle, *J. Geophys. Res.-Solid Earth,* **107**(B4), 2078.

Kennett, B.L.N. & Engdahl, E.R., 1991. Traveltimes for global earthquake location and phase identification, *Geophys. J. Int.,* **105**(2), 429–465.

King, S.D. & Ritsema, J., 2000. African hot spot volcanism: small-scale convection in the upper mantle beneath cratons}, *Science,* **290**(5494), 1137–1140.

Langston, C.A., 1979. Structure under Mount Rainier, Washington, inferred from teleseismic body waves, *J geophys. Res.,* **84**(NB9), 4749–4762.

Lin, S.C. & van Keken, P.E., 2006. Deformation, stirring and material transport in thermochemical plumes, *Geophys. Res. Lett.,* **33**(20).

Montelli, R., Nolet, G., Dahlen, F. & Masters, G., 2006. A catalogue of deep mantle [plumes: new] results from finite-frequency tomography, *Geochem., Geophys. Geosyst.,* **7**(11), Q11007, doi:10.1029/2006GC001248.

Nyblade, A.A. & Brazier, R.A., 2002. Precambrian lithospheric controls on the development of the East African rift system, *Geology,* **30**(8), 755–758.

Nyblade, A.A. & Langston, C.A., 2002. Broadband seismic experiments probe the East African Rift, *EOS, Trans, Am. geophys. Un.,* **278,** 187–209.

Nyblade, A.A., Vogfjord, K.S. & Langston, C.A., 1996. P wave velocity structure of Proterozoic upper mantle beneath central and southern Africa, *J. Geophys. Res.-Solid Earth,* **101**(B6), 13 973–13 973.

Nyblade, A.A., Owens, T.J., Gurrola, H., Ritsema, J. & Langston, C.A., 2000. Seismic evidence for a deep upper mantle thermal anomaly beneath east Africa, *Geology,* **28**(7), 599–602.

Owens, T.J., Nyblade, A.A., Gurrola, H. & Langston, C.A., 2000. Mantle transition zone structure beneath Tanzania, East Africa, *Geophys. Res. Lett.,* **27**(6), 827–830.

Park, Y. & Nyblade, A.A., 2006. P-wave tomography reveals a westward dipping low velocity zone beneath the Kenya Rift, *Geophys. Res. Lett.,* **33**(7), L07311.

Pik, R., Marty, B. & Hilton, D.R., 2006. How many mantle plumes in Africa? The geochemical point of view, *Chem. Geol.,* **226**(3-4), 100–114.

Prodehl, C., Keller, G.R. & Khan, M.A., 1994. Crustal and upper mantle structure of the Kenya Rift, *Tectonophysics,* **236,** 1–488.

Ritsema, J., Nyblade, A.A., Owens, T.J., Langston, C.A. & VanDecar, J.C., 1998. Upper mantle seismic velocity structure beneath Tanzania, east Africa: implications for the stability of cratonic lithosphere, *J. Geophys. Res.-Solid Earth,* **103**(B9), 21 201–21 213.

Ritsema, J., van Heijst, H.J. & Woodhouse, J.H., 1999. Complex shear wave velocity structure imaged beneath Africa and Iceland, *Science,* **286**(5446), 1925–1928.

Sheriff, R., 1980. Nomogram for fresnel-zone calculation, *Geophysics,* **45**(5), 968–972.

Simmons, N.A. & Gurrola, H., 2000. Multiple seismic discontinuities near the base of the transition zone in the Earth's mantle, *Nature,* **405**(6786), 559–562.

Simmons, N.A., Forte, A.M. & Grand, S.P., 2007. Thermochemical structure and dynamics of the African superplume, *Geophys. Res. Lett.,* **34**(2), L02301.

Slack, P.D., Davis, P.M., Dahlheim, H.A., Glahn, A., Ritter, J.R.R., Green, W.V., Maguire, P.K.H. & Meyer, R.P., 1994. Attenuation and velocity of P-waves in the mantle beneath the East-African Rift, Kenya, *Tectonophysics,* **236**(1-4), 331–358.

Tesha, A.L., Nyblade, A.A., Keller, G.R. & Doser, D.I., 1997. Rift localization in suture-thickened crust: evidence from Bouguer gravity anomalies in northeastern Tanzania, East Africa, *Tectonophysics,* **278**(1-4), 315–328.

Vacher, P., Mocquet, A. & Sotin, C., 1998. Computation of seismic profiles from mineral physics: the importance of the non-olivine components for explaining the 660 km depth discontinuity, *Phys. Earth planet. Int.,* **106**(3-4), 275–298.

Vanderlee, S., Paulssen, H. & Nolet, G., 1994. Variability of P660s phases as a consequence of topography of the 660 km discontinuity, *Phys. Earth planet. Int.,* **86**(1-3), 147–164.

Weeraratne, D.S., Forsyth, D.W., Fischer, K.M. & Nyblade, A.A., 2003. Evidence for an upper mantle plume beneath the Tanzanian craton from Rayleigh wave tomography, *J. Geophy. Res.-Solid Earth,* **108**(B9), 2427.